Original Article | Neuroimaging and Head & Neck

http://dx.doi.org/10.3348/kjr.2014.15.6.802
pISSN 1229-6929 · eISSN 2005-8330
Korean J Radiol 2014;15(6):802-809

Korean Journal of Radiology
KJR

Visibility of Sutures of the Orbit and Periorbital Region Using Multidetector Computed Tomography

Hubert Gufler, MD, Markus Preiß, MD, Sabrina Koesling, MD

All authors: Department of Diagnostic Radiology, Martin-Luther-University Halle-Wittenberg, 06120 Halle (Saale), Germany

Objective: Knowledge of cranial suture morphology is crucial in emergency medicine, forensic medicine, and maxillofacial reconstructive surgery. This study assessed the visibility of sutures of the orbit and periorbital region on multidetector computed tomography.

Materials and Methods: Multidetector computed tomography scans of 200 patients (127 males, 73 females; mean age 51.3 years; range, 6–92 years) were evaluated retrospectively. The slice thicknesses varied from 0.5 to 1 mm, and the tube current from 25 to 370 mAs, depending on the CT indication. The visibility of sutures was estimated according to a 4-point scale from "not visible" to "well visible". The chi-squared test was used to test the association of the visibility of sutures with the slice thickness, tube current, and age of patients. Statistical significance was assumed at $p < 0.05$.

Results: Overall, best visibility was found for the sutura frontozygomatica (98%), sutura frontonasalis (88.5%), and sutura sphenozygomatica (71.5%), followed by the sutura zygomaticomaxillaris (65.8%), sutura temporozygomatica (41.8%), sutura frontomaxillaris (44.5%), and sutura sphenofrontalis (31%). Poor visibility was found for the sutura frontolacrimalis (16.8%) and sutura frontoethmoidalis (1.3%). The sutura ethmoidomaxillaris, sutura lacrimomaxillaris, and sutura ethmoidolacrimalis were not visible.

Conclusion: Although the sutures of the superior, lateral, and inferior orbit are well visible, those of the medial orbit are poorly visible on CT scans.

Index terms: *Orbit; Cranial suture; Orbital suture; Computed tomography; Head and neck*

INTRODUCTION

The orbit is a complex cavity confined by seven different bones that are separated from each other by 12 sutures. In contrast to the well-investigated and scientifically described sutures of the cranial vault and skull base, sutures of the orbit and periorbital region have rarely been the focus of imaging studies (1, 2). Most of the existing reports have been limited to skull X-ray studies regarding physiological and premature closure of sutures and age estimates based on suture morphology in forensic medicine. More recently, multidetector computed tomography (MDCT) was used to define the sequence of suture closure for the early diagnosis of skull deformity (2-4). However, no studies have been conducted on the morphology of sutures of the orbit using MDCT *in vivo*. In the emergency setting, it may be challenging to distinguish acute fractures from sutures in the orbital region by CT (5, 6). It would be helpful to know the extent to which sutures of the orbit are visible on MDCT and if visibility is possibly dependent on patient age or on technical parameters (tube current, slice thickness), issues that have not been evaluated so far.

Received November 18, 2013; accepted after revision July 16, 2014.
Corresponding author: Hubert Gufler, MD, Department of Diagnostic Radiology, Martin-Luther-University Halle-Wittenberg, Ernst-Grube-Straße 40, 06120 Halle (Saale), Germany.
• Tel: (49345) 557 2441 • Fax: (49345) 557 2157
• E-mail: hgufler@gmx.de

Korean Journal of Radiology
KJR

The aim of our retrospective study was to analyze CT examinations of the midface and head to assess the visibility of sutures of the orbit and periorbital region.

MATERIALS AND METHODS

Patients

Two hundred consecutive MDCT scans of the midface or head performed in a period of 12 months were analyzed retrospectively. Patients were selected for the study if thin-slice, high-resolution volume data sets could be retrieved from the local picture archiving and communication system. Exclusion criteria were the presence of diseases potentially limiting the evaluation of structures to be analyzed, such as space-occupying processes, osseous damage, or fractures of the orbit and periorbital region.

The main MDCT indications were chronic inflammatory diseases of paranasal sinuses (n = 29) and preoperative navigation for endoscopic endonasal surgery (n = 65) to rule out sequelae of a prior trauma (n = 63), acute complications of inflammation of the midface (n = 37), and others (n = 6).

The age of the patients (73 females, 127 males) ranged from 6 to 92 years (mean age, 51.3 years). Patients were categorized into four age groups: children and adolescents from 6 to 20 years (n = 15), young adults from 21 to 40 years (n = 42), mature adults from 41 to 60 years (n = 64), and older adults of more than 60 years (n = 79).

CT Imaging

Multidetector computed tomography examinations were performed on three different scanners (Sensation 64 and Volume Zoom 4, Siemens Medical Solutions, Forchheim, Germany; Aquilion 32, Toshiba, Otawara, Japan). The slice thicknesses were 0.5 mm (n = 40), 0.6 mm (n = 17), 0.75 mm (n = 37), and 1 mm (n = 106). With the exception of the preoperative navigation protocol, all slices were reconstructed with a 20% to 30% slice overlap. Images were reconstructed with high-resolution convolution kernels: H70s (Sensation 64), FC81 (Aquilion 32), and H60s (Volume Zoom 4). The acquisition matrix was 512 x 512 for all examinations. Typically a field of view of 200 x 200 mm was chosen with a range from 150 x 150 mm for paranasal sinus imaging to 250 x 250 mm for preoperative navigation. The scan range for paranasal sinus imaging included the space from the frontal sinus to the hard palate, for preoperative navigation from the top of the calvarium to the angle of the mandible, and for trauma imaging from the top of calvarium to the hard palate or the mandible. The voltage was 120 kV in each case. According to the tube current employed, four groups were established: 25 to 60 mAs (n = 18), 70 to 75 mAs (n = 133), 125 to 180 mAs (n = 32), and 236 to 370 mAs (n = 17).

Image Assessment

Images were analyzed by two investigators independently on a commercially available workstation (Leonardo Syngo; Siemens Medical Solutions, Forchheim, Germany). Using the original data sets, multiplanar reconstructions were created in any desired plane including standard three orthogonal planes, oblique reformations, and curved reformations. Results were documented on a structured examination

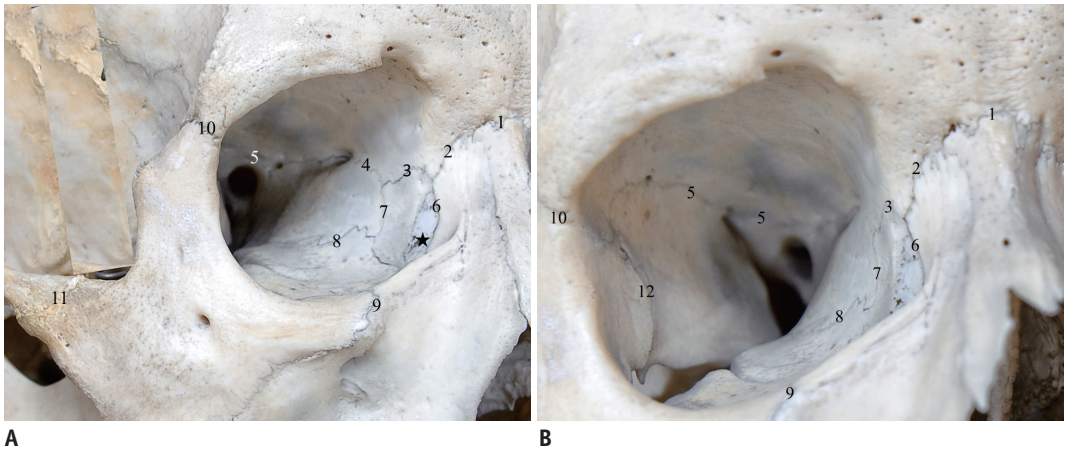

A B

Fig. 1. Two different views on sutures of right orbit and periorbital region.
A. Sutures of medial orbital wall. **B.** Sutures of lateral orbital wall. 1 = sutura frontonasalis, 2 = sutura frontomaxillaris, 3 = sutura frontolacrimalis, 4 = sutura frontoethmoidalis, 5 = sutura sphenofrontalis, 6 = sutura lacrimomaxillaris, 7 = sutura ethmoidolacrimalis, 8 = sutura ethmoidomaxillaris, 9 = sutura zygomaticomaxillaris, 10 = sutura frontozygomatica, 11 = sutura temporozygomatica, 12 = sutura sphenozygomatica. Star = fossa lacrimalis

Table 1. Overall Visibility of Sutures of Orbit and Periorbital Region

Suture	Visibility, n (%)			
	Good	Moderate	Poor	Not Visible
Sutura frontozygomatica	366 (91.5)	17 (4.25)	9 (2.25)	8 (2)
Sutura frontonasalis	120 (60)	31 (15.5)	26 (13)	23 (11.5)
Sutura sphenozygomatica	131 (32.75)	87 (21.75)	68 (17)	114 (28.5)
Sutura zygomaticomaxillaris	70 (17.5)	86 (21.5)	107 (26.75)	137 (34.25)
Sutura temporozygomatica	38 (9.5)	55 (13.75)	74 (18.5)	233 (58.25)
Sutura frontomaxillaris	30 (7.5)	62 (15.5)	86 (21.5)	222 (55.5)
Sutura sphenofrontalis	22 (5.5)	41 (10.25)	61 (15.25)	276 (69)
Sutura frontolacrimalis	6 (1.5)	22 (5.5)	39 (9.75)	333 (83.25)
Sutura frontoethmoidalis	0	0	5 (1.25)	395 (98.75)
Sutura ethmoidomaxillaris	0	0	0	400 (100)
Sutura lacrimomaxillaris	0	0	0	400 (100)
Sutura ethmoidolacrimalis	0	0	0	400 (100)

Note.— n = 200 for sutura frontonasalis and n = 400 for remaining sutures

sheet, which contained time of examination, indication for the examination, and technical parameters (kV, mAs, CT dose indices). Twelve sutures (sutura frontozygomatica, sutura frontonasalis, sutura sphenozygomatica, sutura zygomaticomaxillaris, sutura temporozygomatica, sutura frontomaxillaris, sutura sphenofrontalis, sutura frontolacrimalis, sutura frontoethmoidalis, sutura ethmoidomaxillaris, sutura lacrimomaxillaris, and sutura ethmoidolacrimalis) were evaluated for each side separately, except for the sutura frontonasalis, which was studied only once in each patient (Fig. 1). The visibility of sutures was estimated according to the following 4-point scoring system: not visible = 0, poorly visible = 1, moderately visible = 2, and well visible = 3. If there was a disagreement between the two readers, the decision was reached by consensus. The first investigator had 1 year experience and the second investigator had 25 years of experience in head and neck radiology.

Statistical Analysis

Statistical analysis was performed using the statistical software SPSS version 16 (SPSS Inc., Chicago, IL, USA). The results of statistical analysis of the sutures are expressed both in absolute numbers and percentages. The chi-squared test was used to test for association between the visibility grade of sutures with slice thickness, tube current, and the age of the patients. For chi-squared testing two groups were formed, one consisting of sutures with good or moderate visibility and the other group with poor or absent visibility. Visibilities of sutures in patients aged 6 to 40 years were compared with visibilities in patients aged 41 years and older. Similarly, the visibilities at (summarized) slice thicknesses of 0.5/0.6 mm were compared with visibilities at slice thicknesses of 0.75/1 mm. Finally, summarized visibilities at 25 to 75 mAs were compared with visibilities at 125 to 370 mAs. Statistical significance was assumed for $p < 0.05$.

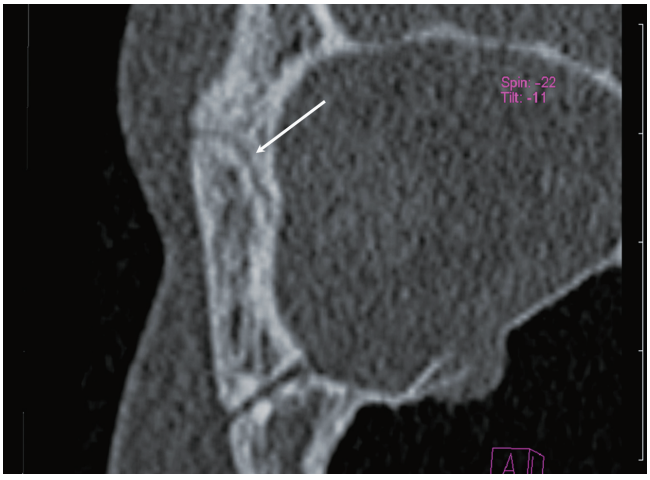

Fig. 2. Sutura frontozygomatica (arrow), coronal multiplanar reconstruction.

RESULTS

Visibility of Sutures on MDCT

Based on 200 MDCT data sets (except for the sutura frontonasalis, 400 orbits), the best visibility (score "well visible") was determined for the sutura frontozygomatica (91.5%), followed by the sutura frontonasalis (60%) and the sutura sphenozygomatica (32.7%) (Table 1, Figs. 2-9). Low visibility was found for sutures of the medial orbital wall merging with the os ethmoidale and os lacrimale.

Korean Journal of Radiology
KJR

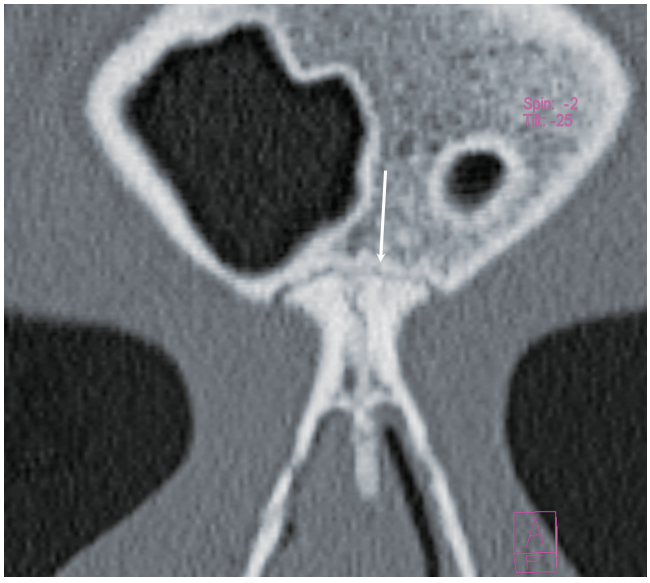

Fig. 3. Sutura frontonasalis (arrow), coronal multiplanar reconstruction.

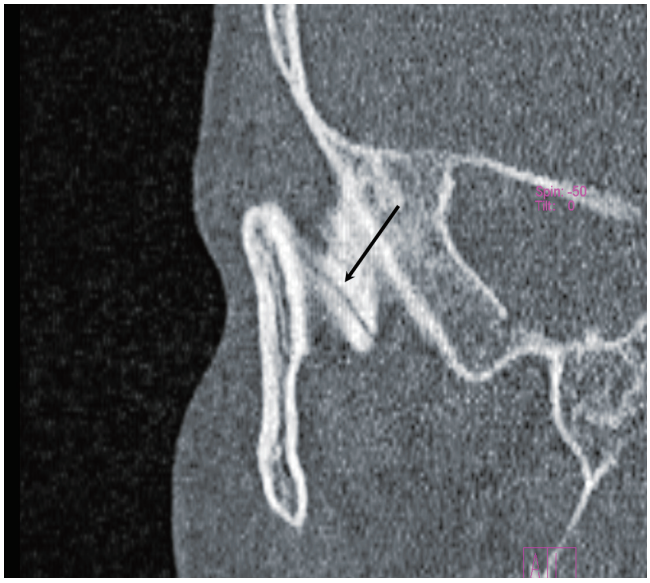

Fig. 4. Sutura sphenozygomatica (arrow), oblique multiplanar reconstruction.

Visibility for the sutura frontolacrimalis was 1.5%; the sutura frontoethmoidalis, sutura ethmoidomaxillaris, sutura lacrimomaxillaris, and sutura ethmoidolacrimalis could not be detected in any case.

Association of the Visibility of Sutures with Slice Thickness

This analysis could not be performed for the sutures merging with the os lacrimale and os ethmoidale due to their low visibility. Apart from the sutura sphenozygomatica and the sutura temporozygomatica, which barely reached

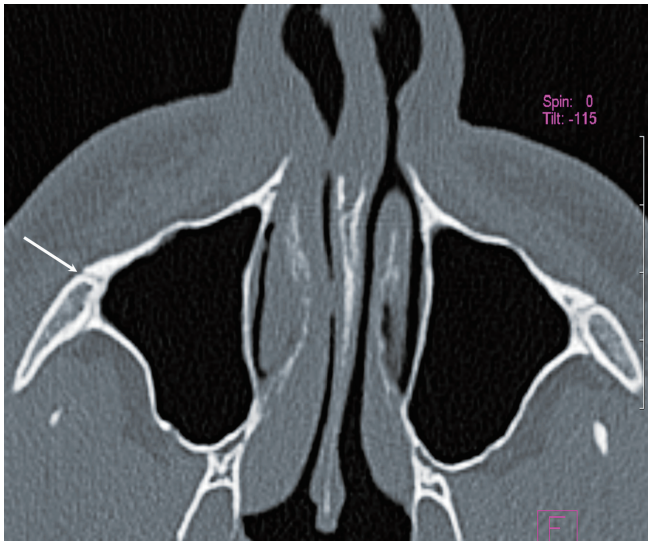

Fig. 5. Sutura zygomaticomaxillaris (arrow), axial CT.

Fig. 6. Sutura temporozygomatica (arrow), axial multiplanar reconstruction.

statistical significance, the association of visibility with slice thickness was statistically significant for all other sutures. In general, the thinner the slices were, the better the visibility of the sutures was (Table 2). The best visibility over all slice thicknesses was observed for the sutura frontozygomatica, which was seen in all cases at a slice thickness of 0.5 mm.

Fig. 7. Sutura frontomaxillaris (arrow), angulated coronal multiplanar reconstruction.

Fig. 8. Sutura sphenofrontalis (solid arrow) and depiction of sutura sphenozygomatica (dashed arrow), angulated coronal multiplanar reconstruction.

Association of the Visibility of Sutures with Tube Current

This analysis could not be performed for the sutures merging with the os lacrimale and os ethmoidale due to their low visibility. Visibility tended to be better at higher doses; however, no statistically significant difference was observed between the groups except for the sutura sphenozygomatica ($p < 0.001$) and the sutura temporozygomatica ($p < 0.02$). Notably, the sutura frontomaxillaris could be seen best (44.4%) at 25 to 60 mAs. The sutura zyogomaticomaxillaris could also be visualized better at lower amperages.

Fig. 9. Sutura frontolacrimalis (arrow), coronal multiplanar reconstruction.

Association of the Visibility of Sutures with Age of Patients

The sutures were best seen at an age of between 6 and 20 years. The sutura frontozygomatica visualization was superior (100%), followed by sutura frontonasalis (86.7%) and sutura zygomaticomaxillaris (73.3%). For these three sutures, no statistically significant difference was found between the different age groups (Table 3). For the other sutures, detection decreased with increasing age, which was statistically significant for the sutura frontolacrimalis, sutura frontomaxillaris, and sutura zygomaticomaxillaris.

As a variant, a sutura frontalis persistens was found in four patients (2%) (Fig. 10).

DISCUSSION

While the sutures of the orbital roof, floor, and lateral wall could be reliably visualized in our study, most of the sutures of the thin part of the medial orbital wall were only

Korean Journal of Radiology
KJR

Table 2. Association of Visibility of Sutures of Orbit and Periobital Region on MDCT with Slice Thickness

Sutures	Slice Thickness				
	0.5 mm n = 80 (%)	0.6 mm n = 34 (%)	0.75 mm n = 74 (%)	1.0 mm n = 212 (%)	*P**
Sutura frontozygomatica	80 (100)	28 (82.35)	72 (97.3)	203 (95.8)	0.0016
Sutura frontonasalis (n = 200)	36 (90)	16 (94.1)	27 (73)	72 (67.9)	0.001
Sutura sphenozygomatica	50 (62.5)	23 (67.7)	40 (54.1)	105 (49.5)	0.055
Sutura zygomaticomaxillaris	46 (57.5)	11 (32.4)	29 (39.2)	70 (33)	0.008
Sutura temporozygomatica	1 (26.3)	11 (32.4)	14 (18.9)	47 (22.2)	0.058
Sutura frontomaxillaris	30 (37.5)	7 (20.6)	19 (25.7)	36 (17)	0.001
Sutura sphenofrontalis	24 (30)	5 (14.7)	5 (6.8)	29 (13.7)	0.001
Sutura frontolacrimalis	12 (15)	0 (0)	6 (8.1)	10 (4.7)	0.597

Note.— n = 200 for sutura frontonasalis and n = 400 for remaining sutures. Comparison of summarized slice thicknesses of 0.5/0.6 mm versus summarized slice thicknesses of 0.75/1 mm. **P* values by chi-squared test

Table 3. Association of Visibility of Sutures with Age of Patients

Sutures	6–20 years n = 30 (%)	21–40 years n = 84 (%)	41–60 years n = 128 (%)	> 60 years n = 158 (%)	*P**
Sutura frontozygomatica	30 (100)	82 (97.6)	120 (93.8)	151 (95.6)	0.448
Sutura frontonasalis	13 (86.7)	31 (73.8)	50 (78.1)	57 (72.2)	0.553
Sutura sphenozygomatica	18 (60)	48 (57.1)	64 (50)	88 (55.7)	0.063
Sutura zygomaticomaxillaris	22 (73.3)	41 (48.8)	48 (37.5)	45 (28.5)	0.001
Sutura temporozygomatica	6 (20)	21 (25)	30 (23.4)	36 (22.8)	0.049
Sutura frontomaxillaris	14 (46.7)	34 (40.5)	15 (11.7)	29 (18.4)	0.001
Sutura sphenofrontalis	8 (26.7)	13 (15.5)	19 (14.8)	23 (14.6)	0.079
Sutura frontolacrimalis	12 (40)	4 (4.7)	6 (4.7)	6 (3.8)	0.001

Note.— n = 200 for sutura frontonasalis and n = 400 for remaining sutures. Comparison of patients aged 6 to 40 years versus patients aged 40 years and older. **P* values by chi-squared test

Fig. 10. Sutura frontalis persistens (arrow), axial scan.

poorly visible or could not be detected. Slice thickness and patient age were the examination variables that influenced visibility significantly. In particular, for the well-visible sutures (sutura frontozygomatica and sutura frontonasalis) and the poorly visible sutures (sutura frontomaxillaris and sutura sphenofrontalis), detectability was best on the thinner slices. A previous CT study of cranial sutures reported this dependency on slice thickness, although the authors used thicker slices of 1.5, 5.0, and 10 mm and did not include orbital sutures (7).

Regarding the dependency of suture visibility on tube current, our results were not uniform. Except for the sutura sphenozygomatica, which could be better visualized at higher amperages, no statistically significant differences could be found for visibility of sutures at different tube currents. It is possible that significantly better results for visibilities may have been achieved for subgroups of patients with combined characteristics, e.g., in adolescents who were examined with thin slices at high amperage. These associations, however, could not be tested by multivariate analysis because of the small sample sizes of subgroups. The results, however, support the already established practice of performing low-dose CT with tube currents of 25 to 50 mAs for bony changes of the skull and midface (8).

From anatomical studies, it is known that the degree of suture closure depends on patient age (2, 7, 9-12). Apart from the sutura frontozygomatica, which begins to close at the age of 28 years, no data exist about the timing of suture closure of the orbit (11). A high variability in time of suture closure in Rhesus monkey skulls has been reported, with a lower grade of ossification of sutures of the midface than of the skullcap (7). Although most of the sutures of the orbit and periorbital region were not mentioned in the study by Wang et al. (9), it can be assumed that the time of suture closure also depends on age for these sutures in humans. This hypothesis could at least partly explain the age dependence of suture visibility in our study. Accordingly, best visibility of sutures was achieved in the youngest age group (6–20 years) of our patients. Over all age groups, visibility was only constantly good for the sutura temporozygomatica. The greatest difference regarding visibility was noted between the age groups 6–20 years and 21–40 years, indicating that sutures probably close at about the time these two periods overlap. Our results also correspond to studies in forensic medicine, where inaccuracy between the estimated and actual age increased with increasing age (10, 12, 13).

Apart from the time of suture closure and CT parameters, there are also good reasons to assume that suture visibility depends on the extent of the area of contact between two adjacent bones. This is corroborated by our study, in which best visibility was obtained for sutures with a broad interface between strong bones, such as the sutura frontozygomatica (visibility, 99%) and sutura frontonasalis (visibility, 88.5%), which are additionally independent of CT parameters. Concerning the sutura zygomaticomaxillaris (visibility, 66%), the sutura temporozygomatica (visibility, 42%), and frontomaxillaris (visibility, 44.5%), the joining bones are admittedly strong; however, the area of contact is smaller than in the aforementioned bones. Although bones are in contact over a long distance, the sutura sphenofrontalis and sutura sphenozygomatica show poor visibility because the involved bones are thin. This applies in particular to sutures of the paper-thin medial orbital wall.

Bademci et al. (6) reported that the sutura frontalis persistens (metopism) represents a potential pitfall when it is mistaken for a fracture line in the emergency setting. The frequency of a sutura frontalis persistens varies in the literature. Of the 200 patients examined in our series, four (2%) showed a sutura frontalis persistens (Fig. 10). Our results are consistent with other reports of a frequency of 1.75% to 3.4% (14-16). A higher variance of this suture from 3.3% to 14.9% has been reported for skulls from an Anatolian provenance across different periods from the Neolithic until the early 20th century (17).

There are several limitations to our study. The retrospective design could have produced selection biases. CT parameters were not uniform for all patients and could not be changed because of the retrospective design of the evaluation. This shortcoming, however, offered the opportunity to compare the results of different examination techniques. The number of patients was distributed heterogeneously, with the youngest age group consisting of only 15 patients; therefore, the statistical power was weak for that group of patients. The unossified sutures in the medial orbit, although narrow and thin, might be seen on CT scans in infants in children younger than 6 years. Poor visibility of sutures of the medial orbital wall may be attributed to the limited spatial resolution of the imaging system, to the small contact areas between these tiny bone structures, and to suture closure. To differentiate poor visibility due to limited resolution of the imaging system from poor visibility due to suture closure, we would need to directly compare the results of MDCT and anatomical examinations. Results can only be compared with those of anatomical studies. With cone-beam CT, thinner slices of 0.125 mm can be achieved, which would probably provide better visibility of sutures of the orbit and periorbital region (18). Finally, it can be speculated as to whether subgroups with combined parameters might have shown significantly better results for visibilities compared to the presented data. This association, however, could not be tested by multivariate analysis because of small sample sizes in the subgroups.

Although the sutures of the superior, lateral, and inferior orbit are well visible, those of the medial orbit are poorly visible on CT scans. The visibility of sutures significantly depends on slice thickness and patient age, but not on tube current. Knowledge of the visibility of orbital sutures on MDCT may be relevant in the emergency setting to distinguish a suture from a fracture line, in reconstructive maxillofacial surgery to detect craniosynostosis, and in forensic medicine to determine age at time of death.

REFERENCES

1. Harth S, Obert M, Ramsthaler F, Reuss C, Traupe H, Verhoff

MA. Ossification degrees of cranial sutures determined with flat-panel computed tomography: narrowing the age estimate with extrema. *J Forensic Sci* 2010;55:690-694
2. Madeline LA, Elster AD. Suture closure in the human chondrocranium: CT assessment. *Radiology* 1995;196:747-756
3. Vannier MW, Pilgram TK, Marsh JL, Kraemer BB, Rayne SC, Gado MH, et al. Craniosynostosis: diagnostic imaging with three-dimensional CT presentation. *AJNR Am J Neuroradiol* 1994;15:1861-1869
4. Sim SY, Yoon SH, Kim SY. Quantitative analysis of developmental process of cranial suture in korean infants. *J Korean Neurosurg Soc* 2012;51:31-36
5. Choudhary AK, Jha B, Boal DK, Dias M. Occipital sutures and its variations: the value of 3D-CT and how to differentiate it from fractures using 3D-CT? *Surg Radiol Anat* 2010;32:807-816
6. Bademci G, Kendi T, Agalar F. Persistent metopic suture can mimic the skull fractures in the emergency setting? *Neurocirugia (Astur)* 2007;18:238-240
7. Furuya Y, Edwards MS, Alpers CE, Tress BM, Ousterhout DK, Norman D. Computerized tomography of cranial sutures. Part 1: comparison of suture anatomy in children and adults. *J Neurosurg* 1984;61:53-58
8. Tack D, Widelec J, De Maertelaer V, Bailly JM, Delcour C, Gevenois PA. Comparison between low-dose and standard-dose multidetector CT in patients with suspected chronic sinusitis. *AJR Am J Roentgenol* 2003;181:939-944
9. Wang Q, Strait DS, Dechow PC. Fusion patterns of craniofacial sutures in rhesus monkey skulls of known age and sex from Cayo Santiago. *Am J Phys Anthropol* 2006;131:469-485
10. Dorandeu A, Coulibaly B, Piercecchi-Marti MD, Bartoli C, Gaudart J, Baccino E, et al. Age-at-death estimation based on the study of frontosphenoidal sutures. *Forensic Sci Int* 2008;177:47-51
11. Todd TW, Lyon DW Jr. Cranial suture closure. Its progress and age relationship. Part II. Ectocranial closure in adult males of white stock. *Am J Phys Anthrop* 1925;8:23-45
12. Mann RW, Jantz RL, Bass WM, Willey PS. Maxillary suture obliteration: a visual method for estimating skeletal age. *J Forensic Sci* 1991;36:781-791
13. Beauthier JP, Lefevre P, Meunier M, Orban R, Polet C, Werquin JP, et al. Palatine sutures as age indicator: a controlled study in the elderly. *J Forensic Sci* 2010;55:153-158
14. Ajmani ML, Mittal RK, Jain SP. Incidence of the metopic suture in adult Nigerian skulls. *J Anat* 1983;137(Pt 1):177-183
15. Agarwal SK, Malhotra VK, Tewari SP. Incidence of the metopic suture in adult Indian crania. *Acta Anat (Basel)* 1979;105:469-474
16. Baaten PJ, Haddad M, Abi-Nader K, Abi-Ghosn A, Al-Kutoubi A, Jurjus AR. Incidence of metopism in the Lebanese population. *Clin Anat* 2003;16:148-151
17. Eroğlu S. The frequency of metopism in Anatolian populations dated from the Neolithic to the first quarter of the 20th century. *Clin Anat* 2008;21:471-478
18. Lagravère MO, Gordon JM, Flores-Mir C, Carey J, Heo G, Major PW. Cranial base foramen location accuracy and reliability in cone-beam computerized tomography. *Am J Orthod Dentofacial Orthop* 2011;139:e203-e210